The voltammetric response of a conical electrode

Artjom V. Sokirko [1], Keith B. Oldham [*]

Department of Chemistry, Trent University, Peterborough, Ont. K9J 7B8, Canada

Abstract

A theoretical study has predicted the course of chronoamperometry following the imposition of a large potential step on an electrode in the shape of an infinite cone, under the usual diffusion-controlled conditions (with diffusivity D). We show how the current density (at a distance r from the apex and at a time t after the step) depends on r^2/Dt and on the semi-apical angle of the cone. The long-time version of this relationship predicts that a cone with a semi-apical angle of 54.74^o will display the unique voltammetric property of independence from D. The short-time relationship throws light on the voltammetric behaviour of vertices in general. © 1997 Elsevier Science S.A.

Keywords: Voltammetry: Conical electrode; Chronoamperometry

1. Introduction

Conical electrodes have been used in hydrodynamic voltammetry, both as rotating cones [1] and in other contexts [2,3]. Recent interest in non-hydrodynamic electrochemistry at conical electrodes has been sparked by the cone being an appropriate model for the rastered tips used in various scanning microscopies [4-9]. The cone electrode has also proved useful in neuroscientific research [lo–121.

Here our interest is in purely diffusive transport to an infinite cone in response to a potential step so large that the concentration at the wall of the cone, initially equal to the uniform value c^b, is diminished instantaneously (at time $t = 0$) to zero. A number of related studies have been made of transport to cones in both electrochemical [2,4,5,13- 15] and non-electrochemical [16– 19] applications, and several more theoretical investigations [20-23] have been conducted as well.

The immediate motivation for the present study was to learn more about the role of vertices in short-time diffusion-controlled chronoamperometry, in concert with other studies carried out in this laboratory [24,25]. We have recently shown, arguing by analogy with the corresponding problem in heat conduction [25,26], that the short-time

current flowing to the walls of a solution-filled hollow cube (of edge length L) in response to a potential leap is

$$I_{cube} = FDc^b \left[\frac{6L^2}{\sqrt{\pi Dt}} - \frac{48L}{\pi} + 96\sqrt{\frac{Dt}{\pi^3}} + \frac{384Dt}{\pi L} \exp\left\{ \frac{-L^2}{16Dt} \right\} - \dots \right] \quad (1)$$

for the case of a one-electron oxidation. Here F is Faraday's constant and D is the diffusivity of the electroactive solute. The first right-hand term is just the cottrellian term arising from the six faces of the cube, each of area L^2. The second right-hand term, the 'prompt' current [24], may be associated with the 12 edges of the cube, each of which contributes a time-independent current of $-4FDc^b L/\pi$. The third right-hand term in this equation arises from the eight vertices of the cube, each of which is seen to contribute a current of $12Fc^b\sqrt{D^3t/\pi^3}$. The fourth and subsequent terms are negligible at short times. The proportionality to $\sqrt{D^3t}$ is characteristic of vertices [24] though, as we shall see later, it also occurs when the electrode has a curved surface. The solid angle in the vertex of a hollow cube is a/2 and it would be of interest to determine how the verticular current depends on the magnitude R of this solid angle and the adjacent geometry. The cone, with its variable apical angle, offers an ideal vehicle for studying this dependence though, as will eventuate in this article, the response of a cone's apex to short-time chronoamper-

ometry does not contribute an unambiguous $\sqrt{D^3 t}$ term in the way that Eq. (I) does for a cube.

Recognise that when we speak of a vertex or an edge 'contributing' a current to the overall faradaic current. we do not mean to imply that these currents actually flow through the vertex or edge [2]. Rather. they are currents that flow to the adjacent faces but they arise because the vertex or edge perturbs the transport conditions there. and their magnitudes reflect the geometry of the vertex or edge.

2. Geometry of the cone

We consider a generalized cone demarcating the boundary between a metal (or other electronic conductor) and an electrolyte solution (or other ionic conductor). The shape of the cone will be characterized by the semi-apical angle θ_0 which is the plane angle *measured in the solution phase* between the axis of symmetry of the cone and its surface, taking values in the $0 < \theta_0 < \pi$ range. What Aoki [13] refers to as a 'spired electrode' corresponds to the smaller range $\pi/2 < \theta_0 < \pi$. In this work. however. attention is equally directed towards the range $0 < \theta_0 < \pi/2$. which corresponds to a 'cavernous electrode' in Aoki's terminology. Cones of the latter geometry have sometimes modelled corrosion pits. The surface separating the metallic and solution phases constitutes the electrode to which a solute species diffuses from the bulk solution. The degenerate case $\theta_0 = \pi/2$, corresponding to the metal|solution boundary being an infinite plane, is not excluded from the treatment. but the designation 'cone' is no longer appropriate.

It is because plane angles are more familiar than their solid counterparts that we use the semi-apical angle θ_0 to characterize the cone's shape, instead of the more fundamental solid angle Ω. The two are related by

$$\Omega = 2\pi(1 - \cos\theta_0) \tag{2}$$

Either of these angles specifies the shape of the cone but. since we are considering the cone to be infinite in extent. no parameter characterizes its size. Applicability of our treatment to finite cones of slant length R is limited to times much smaller than R^2/D, D being the diffusivity of the electroactive solute.

The spherical coordinate system (r, θ, ϕ), as depicted in Fig. 1, provides a convenient framework for investigating diffusion to a cone. The coordinate origin is positioned at the apex of the cone, with the axis of the cone's symmetry corresponding to the latitudinal angle $\theta = 0$ within the solution phase and to $\theta = \pi$ within the metal. The longitudinal angle ϕ is of minor importance here because the cone is symmetrical with respect to rotation through this

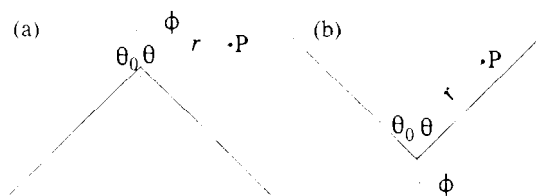

Fig 1   The coordinate system used to designate the position of P. an arbitrary point in solution. In (a) a spired electrode penetrates Into the surrounding solution. $\pi/2 < \theta_0 < \pi$. In (b) the solution occupies the depression in **a** cavernous electrode: $0 < \theta_0 < \pi/2$.

angle. The electrode itself is characterized by $\theta = \theta_0$ and its apex by $r = 0$ where r is the radial coordinate.

3. Concentration distribution

The distribution of temperature in heat-flow problems is strictly analogous to the distribution of solute in diffusion problems. Therefore the solution [27] reported by Carslaw and Jaeger, and obtained by an unpublished Laplace transform derivation. could be adapted to the present problem. However. we present a simpler derivation which does not invoke transforms, relying instead on a dimensional argument to motivate the separation of variables.

A large potential step is applied to the metal at time $t = 0$. whereby the pre-existing equilibrium is perturbed and the concentration of the electroactive species (which has a bulk value c^h) is instantaneously reduced to zero at the electrode surface. Diffusion towards the electrode then ensues in accordance with Fick's second law. which may be written in the simplified spherical coordinate form

$$\frac{1}{D}\frac{\partial c}{\partial t} = \nabla^2 c = \frac{1}{r^2}\frac{\partial}{\partial r}r^2\frac{\partial c}{\partial r} + \frac{\csc\theta}{r^2}\frac{\partial}{\partial\theta}\sin\theta\frac{\partial c}{\partial\theta} \tag{3}$$

that applies when symmetry exists with respect to the longitudinal angle ϕ.

We seek a solution to Eq. (3) subject to the initial condition

$$c = c^h \qquad t = 0. \; r > 0. \; 0 \le \theta \le \theta_0 \tag{4}$$

together with the four boundary conditions

$$c = 0 \qquad t > 0, \; r \ge 0, \; \theta = \theta_0 \tag{5}$$

$$c \to c^h \qquad t > 0. \; r \to \infty, \; 0 \le \theta < \theta_0 \tag{6}$$

$$\frac{\partial c}{\partial\theta} = 0 \qquad t \ge 0, \; r \ge 0, \; \theta = 0 \tag{7}$$

and

$$c = 0 \qquad t > 0, \; r = 0, \; 0 \le \theta < \theta_0, \tag{8}$$

It is convenient. however, to replace all the independent variables $(t, \; r \text{ and } \theta)$ before proceeding to solve the differential equation.

---

[2] A negative contribution would then be impossible.

The resolution of the problem posed by this set of equations is aided by recognising that. other than c itself. the only quantities with physical dimensions in our problem are t. r and D. It then follows from dimensional considerations that the solution must be of the form

$$\frac{c}{c^b} = f\left\{\frac{r^2}{Dt}, \theta\right\} = f\{\xi, \theta\} = F\{\xi, \cos\theta\} = F\{\xi, \mu\} \quad (9)$$

where ξ is the dimensionless composite r^2/Dt, f being the sought function of that composite and of the latitudinal angle θ. It will transpire that $\cos\theta$, which we temporarily abbreviate to μ, is a more convenient variable than θ itself, which motivates the replacement of the function $f\{\xi, \theta\}$ by $F\{\xi, \mu\}$. Let us further assume separability of the new independent variables, i.e. that a product $c/c^b = F\{\xi, \mu\} = \Xi\{\xi\}U\{\mu\}$ of separate functions of the variables will satisfy the differential equation (3). In practice, we expect that an infinity of such products will satisfy the differential equation, but that a specific linear combination of them

$$\frac{c}{c^b} = F\{\xi, \mu\} = \sum_{n=1}^{\infty} w_n \Xi_n\{\xi\} U_n\{\mu\} \quad (10)$$

will be needed to satisfy the boundary conditions also. Here each Ξ_n is a function of ξ but not of μ and each U_n, is a function of μ but not of ξ. The presently unspecified factors w_n permit suitable weights to be assigned to the $\Xi_n\{\xi\}U_n\{\mu\}$ products to match the boundary conditions.

Each individual $\Xi_n\{\xi\}, U_n\{\mu\}$ pair must satisfy the differential equation (3), which becomes

$$\frac{\xi}{\Xi_n}\left[4\xi \frac{d^2\Xi_n}{d\xi^2} + (\xi + 6)\frac{d\Xi_n}{d\xi}\right]$$

$$= \frac{-1}{U_n}\left[(1 - \mu^2)\frac{d^2U_n}{d\mu^2} - 2\mu\frac{dU_n}{d\mu}\right] \quad (11)$$

after incorporation of Eq. (10), along with the definitions of ξ and μ. Similarly, conditions (4)–(8) become

$$\sum_{n=1}^{\infty} w_n \Xi_n\{\xi\} U_n\{\mu\} \to \infty \qquad \xi \to \infty, \mu_0 < \mu \le 1 \quad (12)$$

$$\sum_{n=1}^{\infty} w_n \Xi_n\{\xi\} U_n\{\mu\} = 0 \qquad 0 < \xi < \infty, \mu = \mu_0 \quad (13)$$

$$\sum_{n=1}^{\infty} w_n \Xi_n\{\xi\} \frac{dU_n\{\mu\}}{d\mu} \neq \infty \qquad 0 \le \xi < \infty, \mu = 1 \quad (14)$$

and

$$\sum_{n=1}^{\infty} w_n \Xi_n\{\xi\} U_n\{\mu\} = 0 \qquad \xi = 0, \mu_0 < \mu \le 1 \quad (15)$$

in terms of the new dependent and independent variables. where $\mu_0 = \cos\theta,$[3].

The left-hand side of Eq. (11) is a function only of ξ, whereas the right-hand side depends only on μ. It follows that each side must equal the same constant, say k_n. Looking first at the right-hand side, we have

$$(1 - \mu^2)\frac{d^2U_n}{d\mu^2} - 2\mu\frac{dU_n}{d\mu} + k_n U_n = 0 \quad (16)$$

This resembles the standard form of Legendre's equation [28] and its solution is in terms of Legendre functions of argument μ and of a degree υ_n that is related to the separation constant k_n

$$U_n\{\mu\} = b_n P_{\upsilon_n}\{\mu\} + b_n' Q_{\upsilon_n}\{\mu\} \quad \text{where}$$

$$\upsilon_n = -(1/2) \pm \sqrt{k_n + (1/4)} \quad (17)$$

where arbitrary constants are represented by b_n and b_n'. The second of these, however, must be zero because boundary condition (14) would otherwise be violated on the symmetry axis, $Q_{\upsilon}\{\mu\}$ and its derivative being unbounded for all υ when $\mu = 1$. Because no choice has yet been made for the weights w_n in Eq. (10), we are free to choose any non-zero value that we wish for b_n and unity will be chosen. Hence

$$U_n\{\mu\} = P_{\upsilon_n}\{\mu\} \quad (18)$$

each U_n function corresponding to a distinct value of υ_n. Because $P_{-\upsilon_n-1}\{\mu\} = P_{\upsilon_n}\{\mu\}$, we need consider only $\upsilon_n \le -1/2$, or $\upsilon_n \ge -1/2$, and the latter option will be selected.

Now, turning to the left-hand side of Eq. (11) with k_n appropriately replaced by $\upsilon_n(\upsilon_n + 1)$, we have

$$4\xi^2\frac{d^2\Xi_n}{d\xi^2} + (\xi^2 + 6\xi)\frac{d\Xi_n}{d\xi} - \upsilon_n(\upsilon_n + 1)\Xi_n = 0 \quad (19)$$

Standard methods [29] show that the solution of this ordinary differential equation is

$$\Xi_n\{\xi\} = B_n \xi^{\frac{\upsilon_n}{2}} M\left\{\frac{\upsilon_n}{2}; \upsilon_n + \frac{3}{2}; \frac{-\xi}{4}\right\}$$

$$+ B_n' \xi^{\frac{-\upsilon_n-1}{2}} M\left\{\frac{-\upsilon_n-1}{2}; \frac{1}{2} - \upsilon_n; \frac{-\xi}{4}\right\} \quad (20)$$

where M{ : : } denotes a Kummer function [30] [4]. B_n and

---

[3]Notice that $\mu_0 = (2\pi - \Omega)/2\pi$ and that, since $\Omega = 2\pi$ corresponds to a plane, we expect the voltammetric effects of a vertex to depend on the difference $2\pi - \Omega$, and hence, in some simple way. on μ_0.

[4]Also known as a 'confluent hypergeometric function' or 'degenerate hypergeometric function'. Alternative notations are $\Phi\{::\}$ and $_1F_1\{;;\}$.

B'_n are arbitrary but the latter must be zero to avoid violation of boundary condition (15) when $\xi = 0$. As with b_n in the preceding paragraph, we are free to select $B^n = 1$.

At this stage, the solution to our problem is

$$\frac{c}{c^b} = \sum_{n=1}^{\infty} w_n P_{v_n}\{\mu\} \xi^{\frac{v_n}{2}} M\left\{\frac{v_n}{2}; v_n + \frac{3}{2}; \frac{-\xi}{4}\right\} \qquad (21)$$

and all that is required is the selection of an appropriate set of v_n values and a corresponding set of weights w_n to satisfy the boundary conditions. To satisfy condition (13) it suffices to choose v_n to be the nth positive value of v [5] that makes $P_v\{\mu_0\}$ equal to zero [6], for then each summand in Eq. (21) becomes zero at $\mu = \mu_0$. In addressing condition (12), we first observe [31] that

$$\xi^{\frac{v_n}{2}} M\left\{\frac{v_n}{2}; v_n + \frac{3}{2}; \frac{-\xi}{4}\right\} \rightarrow 2^v \frac{\Gamma\left\{v + \frac{3}{2}\right\}}{\Gamma\left\{\frac{v}{2} + \frac{3}{2}\right\}} \text{ as } \xi \rightarrow \infty \qquad (22)$$

so that

$$\sum_{n=1}^{\infty} w_n P_{v_n}\{\mu\} 2^{v_n} \frac{\Gamma\left\{v_n + \frac{3}{2}\right\}}{\Gamma\left\{\frac{v_n}{2} + \frac{3}{2}\right\}} = 1 \text{ for } \mu_0 < \mu \leq 1 \qquad (23)$$

becomes a redrafting of boundary condition (12).

To evaluate the weights, we make use of the orthogonality property [32] that

$$\int_{\mu_0}^{1} P_{v_n} P_{v_N} \, d\mu = \begin{cases} 0 & \text{if } N \neq n \\ \dfrac{-(1-\mu_0^2)p_n q_n}{2v_n + 1} & \text{if } N = n \end{cases} \qquad (24)$$

Here p_n and q_n are partial derivatives of the P_{v_n} Legendre function with respect to degree and argument respectively [7]. The former,

$$P_n = \left[\frac{\partial P_v\{\mu_0\}}{\partial v}\right]_{v = v_n} \qquad (25)$$

cannot be expressed usefully in simpler terms, but the latter can be related to a Legendre function of changed degree

$$q_n = \left[\frac{\partial P_{v_n}\{\mu\}}{\partial \mu}\right]_{\mu = \mu_0} = \frac{v_n P_{v_n - 1}\{\mu_0\}}{1 - \mu_0^2} \qquad (26)$$

Now, if each side of Eq. (23) is multiplied by $P_{v_N}\{\mu\}$, where the degree v_N is some specific choice of v_n, and integration is performed over $\mu_0 < \mu < 1$, then the orthogonality ensures that all but one of the summands disappear. There remains

$$-(1-\mu_0^2) w_N p_N q_N 2^{v_N - 1} \frac{\Gamma\left\{v_N + \frac{1}{2}\right\}}{\Gamma\left\{\frac{v_N}{2} + \frac{3}{2}\right\}} = \int_{\mu_0}^{1} P_{v_N}\{\mu\} \, d\mu \qquad (27)$$

The integral may be evaluated in terms of the quantity in definition (26) [8].

$$\int_{\mu_0}^{1} P_{v_N}\{\mu\} \, d\mu = \frac{(1-\mu_0^2)}{v_N(v_N + 1)} \left[\frac{\partial P_{v_N}\{\mu\}}{\partial \mu}\right]_{\mu = \mu_0}$$

$$= \frac{(1-\mu_0^2)}{v_N(v_N + 1)} q_N \qquad (28)$$

Accordingly, by combining the last two equations, we arrive, after some algebra, at the expression

$$w_N = \frac{-\Gamma\left\{\dfrac{v_N}{2} + \dfrac{1}{2}\right\}}{2^{v_N} v_N \Gamma\left\{v_N + \dfrac{1}{2}\right\} p_N} \qquad (29)$$

for the Nth weight.

Now that the weights are evaluated, Eqs. (21) and (29) may be combined. The final result, giving the concentration at all points in the electrolyte solution at all times subsequent to the potential leap, is

$$c = -c^b \sum_{n=1}^{\infty} \left(\Gamma\left\{\frac{v_n}{2} + \frac{1}{2}\right\} P_{v_n}\{\cos\theta\} \left(\frac{r^2}{4Dt}\right)^{\frac{v_n}{2}} M\left\{\frac{v_n}{2}; v_n + \frac{3}{2}; \frac{-r^2}{4Dt}\right\} \right. \\ \left. \Big/ v_n \Gamma\left\{v_n + \frac{1}{2}\right\} \left[\frac{\partial P_v\{\cos\theta_0\}}{\partial v}\right]_{v = v_n} \right) \qquad (30)$$

after the original variables are restored. Carslaw and Jaeger [27] report a different, but demonstrably equivalent, solution to the corresponding problem in heat conduction. As a further check for the correctness of this formula, the $\theta_0 = \pi/2$ case was shown to conform [33] to the well-known error function complement solution [34] for the infinite plane.

---

[5] Suitable values of the degree should be sought in the range $v \geq -1/2$, but there exist no values in $-1/2 \leq v \leq 0$ that generate zeros of $P_v\{\mu\}$.

[6] For example, v_1 and v_2 approximate 1.777 and 3.763 respectively if $\mu_0 = 1/2$, whereas $v_1 \approx 0.6015$ and $v_2 \approx 2.113$ if $\mu_0 = -1/2$. When μ_0 is negative (i.e. for $\pi/2 < \theta_0 < \pi$) then $v_1 < 1$, whereas $v_1 > 1$ for positive μ_0.

p_1 is negative, q_1 is positive. As n increments, both p_n and q_n alternate in sign. Hence both the product $p_n q_n$ and the quotient q_n/p_n are invariably negative.

[8] To prove this, Integrate Legendre's equation in the form $v(v + 1)P_v\{\mu\} = (1-\mu^2)d^2 P_v\{\mu\}/d\mu^2 - 2\mu dP_v\{\mu\}/d\mu = d[(1-\mu^2)dP_v\{\mu\}/d\mu]/d\mu$; then set $v = v_n$ and $\mu = \mu_0$.

It is convenient to adopt the abbreviation

$$g_n = 2^{v_n} w_n q_n = \frac{-\Gamma\left\{\dfrac{v_n}{2} + \dfrac{1}{2}\right\} q_n}{v_n \Gamma\left\{v_n + \dfrac{1}{2}\right\} p_n} \tag{31}$$

because this, grouping of terms occurs frequently in what follows.

4. Current distribution

Using Laplace and Lebedev-Kontorovich transform, Aoki [13] derived the current distribution on the surface of an infinite cone. Here we follow an alernative route. starting with Eq. (30).

If we suppose the electrode reaction to be a one-electron oxidation of the electroactive diffusant [9]. then the current density i at any point on the surface of the conical electrode is proportional to the flux density j of the diffusant there and hence. via Fick's first law, to the local concentration gradient

$$i = -Fj_{\theta=\theta_0} = FD\left[\frac{\partial c}{\partial n}\right]_{\theta=\theta_0} \tag{32}$$

n now denotes the dimension normal to the electrode surface. Small lengths dn measured along this normal equal $-r\,d\theta$. or equivalently $r\,d\mu/\sqrt{1-\mu^2}$. Accordingly, we find

$$i = \frac{FD\sqrt{1-\mu_0^2}}{r}\left[\frac{\partial c}{\partial \mu}\right]_{\mu=\mu_0}$$

$$= \frac{FDc^b \sin\theta_0}{r} \sum_{n=1}^{\infty} g_n \left(\frac{r^2}{4Dt}\right)^{\overline{2}} M\left\{\frac{v_n}{2} : v_n + \frac{3}{2} : \frac{-r^2}{4Dt}\right\}$$

$$= i_{\text{cone}} \tag{33}$$

the second step incorporating the result of differentiation of Eq. (30). Though its implication\ are rather opaque. Eq. (33) is an exact expression for the faradaic current density. valid at all times and at each location on the conical surface. Though couched in different terminology (note that his θ_0 differs from ours. the two iumming to π: his $\mu_{k-1/2}$ corresponds to our v_n) the 1990 solution of Aoki [13] has been shown [35] to be equivalent to Eq. (33).

It will have been observed that, unlike the concentration distribution, in which the dependences on radial distance and time are inextricably conjoined in the composite variable r^2/Dt. the presence of the denominatorial 'r' outside the summation in Eq. (33) means that the current density
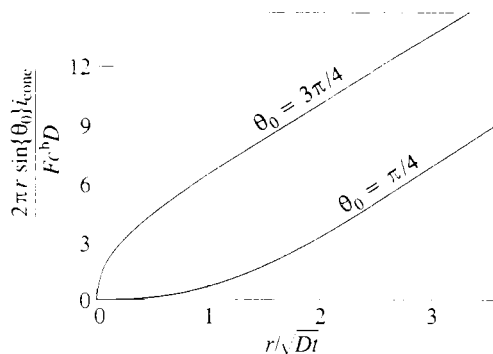

Fig. 2. The product of current density and perimeter length, normalised by division by Fc^bD. at a distance r from the apex of a cone, plotted as a function of $r/\sqrt{Dt}$ for the semi-apical angles $\theta_0 = 3\pi/4$ and $\pi/4$.

has uconstrained dependences on r and t. This is a disadvantage when it comes to presenting our results in tabular or graphical form. A remedy is to compute the product of the current density and the local circumference of the cone. i.e.

$$2\pi r \sin\{\theta_0\} i_{\text{cone}} = 2\pi FDc^b \sin^2\{\theta_0\} \sum_{n=1}^{\infty} g_n \left(\frac{r^2}{4Dt}\right)^{\overline{2}}$$

$$\times M\left\{\frac{v_n}{2} : v_n + \frac{3}{2} : \frac{-r^2}{4Dt}\right\} \tag{34}$$

The right-hand side of this expression is a function only of the r^2/Dt composite variable and of θ_0. Fig. 2 shows the form of this function for representative values. namely $3\pi/4$ and $\pi/4$. of the semi-apical angle θ_0.

In principle, integration of Eq. (34) can give the total current tlouing to a segment (say the segment $0 < r < R$) of the cone:

$$I = 2\pi \sin\theta_0 \int_0^R r i_{\text{cone}} \, dr \tag{35}$$

with i_{cone} denoting the expression given in Eq. (33) for the current density. However, our attempts to evaluate the integral formulated in Eq. (35) analytically have failed. Nevertheless, the integration could be carried out numerically for chosen values of θ_0 and R. using procedures similar to those reported in a later section of this article. Such an integration would yield the current flowing to a segment of an infinite cone. not that corresponding to a finite cone of slant length R. Of course, the current is infinite when ∞ replaces R as the upper limit in Eq. (35).

We next discuss some limiting cases and examples.

5. Long-time behaviour

As expected, the current density is infinite everywhere immediately following the potential leap. It remains infinite at the cone's apex if $\theta_0 > \pi/2$, but not otherwise. To demonstrate this. consider the form adopted by Eq. (33) as

---

[9] For an n-electron oxidation multipliy all current and current density expressions by n; for an n-electron reduction multiply by $-n$

$r \to 0$. For small values of its $r^2/4Dt$ argument. the Kummer function adopts a value close to unity and. because of the term $(r^2/4Dt)^{\iota_n/2}$, the summation comes to be dominated by its early members. so that

$$i_{cone} = \frac{FDc^b \sin \theta_0}{r} \left[g_1 \left(\frac{r^2}{4Dt} \right)^{\frac{\iota_1}{2}} + g_2 \left(\frac{r^2}{4Dt} \right)^{\frac{\iota_2}{2}} + \dots \right]$$

(36)

and this becomes

$$i_{cone} \to \frac{Fc^b \sin \theta_0 g_1 D^{1-\frac{\iota_1}{2}} r^{\iota_1 - 1}}{2^{\iota_1} t^{\frac{\iota_1}{2}}} \quad \text{as} \quad \frac{r^2}{Dt} \to 0$$

(37)

in the limit.

As reported in footnote 3, ι_1 is less than unity when $\theta_0 > \pi/2$, so that r has a negative exponent in Eq. (37) under this circumstance, and hence $i \to \infty$ as $r \to 0$. An example is provided by the cone illustrated in Fig. 1(a) with $\theta_0 = 3\pi/4$. For this semi-apical angle, $\iota_1 = 0.4631$, from which we calculate that the current density is

$$i_{\theta_0 = 3\pi/4} = 0.9207 Fc^b D^{0.7685} r^{-0.5369} t^{-0.2315}$$

$$\text{when } r^2 \ll Dt$$

(38)

On the contrary, when θ_0,, is smaller than a right angle, ι_1 exceeds unity and the positive exponent that r then acquires implies that the current density tends to zero as the cone's apex is approached. The numerical parameters in the equation

$$i_{\theta_0 = \pi/4} = 0.11624 Fc^b D^{-0.2739} r^{1.5479} t^{-1.2739}$$

$$\text{when } r^2 \ll Dt$$

(39)

were calculated for the angle $\theta_0 = \pi/4$, the case illustrated in Fig. 1(b), for which $\iota_1 = 2.5479$. These behaviours are exactly as might have been expected intuitively, when one considers the respective ease and difficulty of access by the diffusant to the apex of cones with obtuse and acute semi-apical angles.

Eqs. (38) and (39) represent typical examples of currents at spired and cavernous electrodes respectively. In the preceding paragraph we interpreted these equations as reflecting the dependence of the current density, at some constant time after the potential leap, on the coordinate r which, in the present context, represents small slant lengths measured from the apex of the cone. Equally, these equations describe how the current density, at a fixed site on the cone, depends on time. In this interpretation, the equations are valid only at times long enough that $t \gg r^2/D$. Thus, *at* that apex, the equations are valid immediately, but longer and longer waiting times must elapse before applicability spreads away from the apex along the sides of the cone.

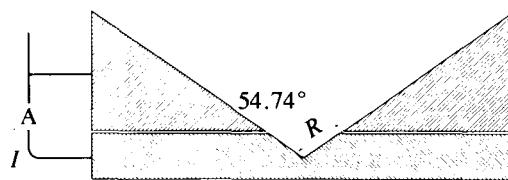An interesting special case arises when the semi-apical

Fig. 3. Diagram of a device that will give a long-time current response independent of the diffusivity of the electroactive species hut proportional to its concentratlon.

angle [10] is $54.7356°$ (i.e. arcsec $\sqrt{3}$), for then the long-time current density is proportional to r, inversely proportional to t, and totally independent of the diffusivity of the electroactive species:

$$i_{\theta_0 = \pi/3.2885} = \frac{0.2212 Fc^b r}{t} \quad \text{when } r^2 \ll Dt$$

(40)

This behaviour has implications for chemical analysis, because the voltammetric signal in this circumstance is independent of the nature of the analyte yet accurately proportional to its concentration. There are circumstances in which this could be advantageous. Consider, for example. the problem of determining the total concentration of a number of homologues, organic amines for example, all present in a sample and oxidizing at about the same potential, but having different diffusivities. A diffusivity-independent technique could yield this information, whereas the analysis could not easily be accomplished by regular voltammetric techniques, even if the diffusion coefficients were known. Though the fabrication of such a device of sufficiently miniature size might be taxing, one way in which the diffusivity-independent property might be exploited is illustrated in Fig. 3. A cavernous conical working electrode of semi-apical angle 54.74" contains the analyte solution and has two parts separated by a very narrow insulating annulus. The upper portion of the working electrode serves only as a 'guard' to ensure that the equi-concentration surfaces adjacent to the lower portion are those appropriate to an infinite cone. Though the same potential-leap signal is applied to both portions of the working electrode, only the current flowing to the lower portion is monitored. The current flowing to the lower portion, after the passage of sufficient time to ensure that $t \gg R^2/D$, is

$$I = 0.2212 Fc^b \int_0^R \frac{2\pi \sin(54.74) r}{t} dr = \frac{0.5674 Fc^b R^2}{t}$$

(41)

where R is the slant height of the lower portion of the working electrode, as illustrated in Fig. 3. It is very

[10] The apical angle $2\theta_0$ is then the 'tetrahedral angle' of organic chemistry.

unusual to encounter a diffusion-mediated voltammetric current that, as here, is independent of the diffusivity of the electroreactant. The paradox arises in this special case because a large diffusivity favours a small reactant concentration in the surface layers adjacent to the apex. but at the same time also favours a large flux through those surface layers; the two effects exactly compensate for this particular semi-apical angle.

6. Short-time behaviour

By 'short-time' we mean $t \ll r^2/D$, so that short-times' endure for long periods at points on the cone remote from the apex, but are ephemeral close to the apex. The phrase 'short-times at the apex' is meaningless; at the apex all times are 'long'.

The limiting cases considered in the last section relate to long times such that $r^2 \ll Dt$. When we turn to the converse limit of times small in comparison with r^2/D, we can be confident that the Cottrell relationship

$$i = Fc^b \sqrt{\frac{D}{\pi t}} \quad \text{when } r' \gg Dt \quad (42)$$

will hold. In the light of Eq. (33), this implies that

$$\sum_{n=1}^{\infty} g_n \left(\frac{\xi}{4} \right)^{t_n/2} M \left\{ \frac{t_n}{2}; t_n + \frac{3}{2}; \frac{-\xi}{4} \right\} \to \frac{\sqrt{\xi}}{\sqrt{\pi}(1-\mu^2)}$$
$$\text{as } \xi \to 0 \quad (43)$$

but, despite diligent attempts. we have been unable to establish this behaviour either mathematically or computationally [11]. Our confirmation that Eq. (43) is. indeed. correct is made in the circuitous fashion discussed in the next section.

7. Comparison with a cylinder

In the absence of a useful analytical short-time expression for the current at a cone with which to compare our numerical results, we have chosen to make a comparison with the current density at an electrode of more tractable shape, the cylinder. Unlike the case of the cone. two very distinct solutions apply to chronoamperometry at a cylindrical electrode according to whether diffusion occurs inside or outside the cylindrical surface. In response to a potential leap, the current density at an electrode occupying the surface of an infinite cylindrical metal rod of radius a is [36.37]

$$i = \frac{4FDc^b}{\pi^2 a} \int_0^\infty \frac{\exp(-\lambda^2 Dt/a^2)}{\lambda J_0^2\{\lambda\} + \lambda Y_0^2\{\lambda\}} \, d\lambda \quad (44)$$

whereas the corresponding current density on an electrode occupying the inner surface of an infinite cylindrical metal tube of the same radius [38.39] is

$$i = \frac{2FDc^b}{a} \sum_{n=1}^\infty \exp\left\{ \frac{-\beta_n^2 Dt}{a^2} \right\} \quad (45)$$

In these equations $Y_0\{\}$ denotes the zero-order Neumann function [40], $J_0\{\}$ is the zero-order Bessel function [41] and β_n is the nth zero of the latter function [42].

The mean curvature [24] of a cylinder has a constant value. $H = 1/2a$ for the outside case and $H = -1/2a$ for the inside case, whereas the mean curvature of a cone varies with r, being given by $H = -\cot\theta_0/2r$ irrespective of whether the curvature is positive or negative. Accordingly. the best match of a cylinder to a cone is obtained by replacing n in Eq. (44) by $-r/\cot\theta_0$ and in Eq. (45) by $r/\cot\theta_0$. Hence the current density

$$i_{\text{model}}$$
$$= \begin{cases} \dfrac{2FDc^b \cot\theta_0}{-} \displaystyle\sum_{n=1}^\infty \exp\left\{ \dfrac{-\beta_n^2 \cot'\{\theta_0\} Dt}{r^2} \right\} & 0 < \theta_0 < \dfrac{\pi}{2} \\[4mm] \dfrac{-4FDc^b \cot\theta_0}{\pi^2 r} \displaystyle\int_0^\infty \dfrac{\exp\{-\cot^2\{\theta_0\}\lambda^2 Dt/r^2\}}{\lambda J_0^2\{\lambda\} + \lambda Y_0^2\{\lambda\}} \, d\lambda & \dfrac{\pi}{2} < \theta_0 < \pi \end{cases}$$
$$(46)$$

can be ascribed to the 'cylindrical model' of a cone. Recognise that this model does not correspond to any actual physical body: we have taken the faradaic properties of a cylinder and grafted some of the curvature properties of a cone onto it.

Our next task is to compare the total current at the infinite cone to that of the cylindrical model by evaluating the difference

$$\Delta I = I_{\text{cone}} - I_{\text{model}} = 2\pi \sin\theta_0 \int_0^\infty (i_{\text{cone}} - i_{\text{model}}) r \, dr \quad (47)$$

Note that the individual currents I_{cone} and I_{model} are both infinite. so that to obtain finite values of ΔI is a stringent test not only of the theory, but also of the numerical procedures that were needed to evaluate expression (47) numerically. Of course we do not expect to find $\Delta I = 0$, because a cone possesses features that an assemblage of cylindrical elements lacks. To aid the integration in Eq. (47) it is convenient to reintroduce the $\xi = r^2/Dt$ variable.

---

[11] Note that the incorporation of the asymptotic formula (19) directly into Eq. (29) leads to the erroneous conclusion that the current denaity should be inversely proportional to r and independent of r. Evidently the presence of terms involving t_n,
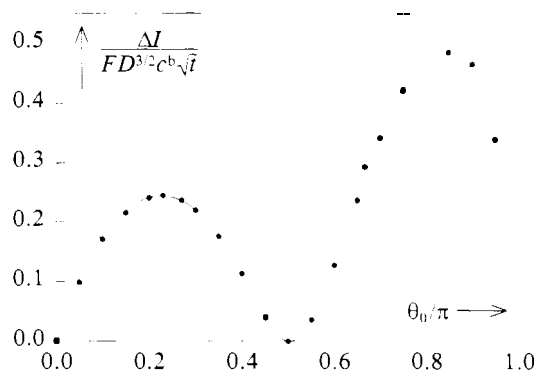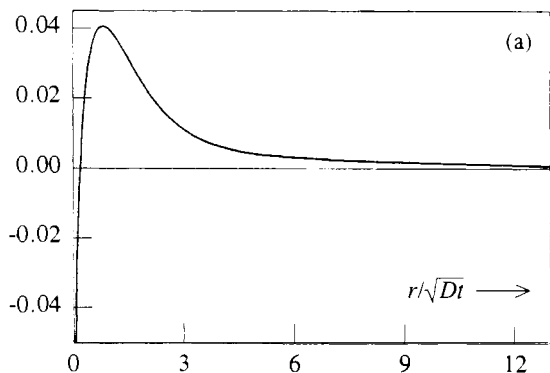
Fig. 1. Graph. versus the semi-apical angle θ_0. of the difference between the current at an infinite cone and that at the cylindrical model of an infinite cone. The current difference increases with time and has been normalised by division by $FD^{3/2}c^b/\sqrt{t}$.

Thereby, the expression for the normalised current difference becomes

$$\frac{\Delta I}{FD^{3/2}c^b\sqrt{t}} = \int_0^\infty \left[\frac{4\mu_0}{\pi\sqrt{\xi}} \int_0^\infty \frac{\exp\{-\mu_0^2\lambda^2/(1-\mu_0^2)\xi\}}{\lambda J_0^2\{\lambda\} + \lambda Y_0^2\{\lambda\}} \, d\lambda \right.$$

$$\left. + \frac{\pi}{2} \sum_{n=1}^\infty \left(1-\mu_0^2\right)\left(\frac{\xi}{4}\right)^{\frac{v_n}{2}-\frac{1}{2}} M\left\{\frac{v_n}{2} : v_n + \frac{3}{2} : \frac{-\xi}{4}\right\} \right] d\xi$$

$$(48)$$

for the $\pi/2 < \theta_0 < \pi$ case. The results of a numerical integration of this formula. and of the similar but less elaborate formula

$$\frac{\Delta I}{FD^{3/2}c^b\sqrt{t}} = \int_0^\infty \sum_{n=1}^\infty \left[\frac{-2\pi\mu_0}{\sqrt{\xi}} \exp\left\{\frac{-\beta_n^2\mu_0^2}{(1-\mu_0^2)\xi}\right\} \right.$$

$$+ \frac{\pi}{2} g_n\left(1-\mu_0^2\right)\left(\frac{\xi}{4}\right)^{\frac{v_n}{2}-\frac{1}{2}}$$

$$\left. \times M\left\{\frac{v_n}{2} : v_n + \frac{3}{2} : \frac{-\xi}{4}\right\} \right] d\xi \qquad (49)$$

that applies when $0 < \theta_0 < \pi/2$. are displayed in Fig. 4 for almost the entire range of semi-apical angles. Gratifyingly. the magnitude of ΔI is not only finite but surprisingly modest. Observe that ΔI is proportional to $\sqrt{t}$. so that as $t \to 0$ the difference between the current at the cone and that at its cylindrical model vanishes. We regard this as confirmation of limit (43) and, by extension. as a vindication of Eq. (33).

Fig. 4 shows that, as expected. the difference between the currents is zero at $\theta_0 = \pi/2$, for which angle both the cone and its cylindrical model reduce to an infinite plane. ΔI is shown as being zero for $\theta_0 = 0$ and appears to be approaching a zero limit as $\theta_0 \to \pi$, but the calculations become unstable as those end values are approached and we have less confidence in our knowledge of the behaviours of the cone and its model in those extremities.

The curve in Fig. 4 was constructed by interpolating the data points shown. Each point is the result of graphical integration of a curve. of which examples are portrayed in Fig. 5.

8. Short-time behaviour revisited

The short-time voltammetric response of a cylinder of radius a is captured by the equation

$$i_{cyl} = FDc^b\left[\frac{1}{\sqrt{\pi Dt}} \pm \frac{1}{2a} - \frac{1}{4a^2}\sqrt{\frac{Dt}{\pi}} \right.$$

$$\left. \pm \frac{Dt}{8a^3} - O\left\{\frac{(Dt)^{3/2}}{a^4}\right\} \right] \qquad (50)$$

where the upper sign relates to the outside of the cylinder and the lower to the inside [24]. In building the model, we replaced $\pm 1/2a$ by $-\cot\theta_0/2r$, so that the short-time
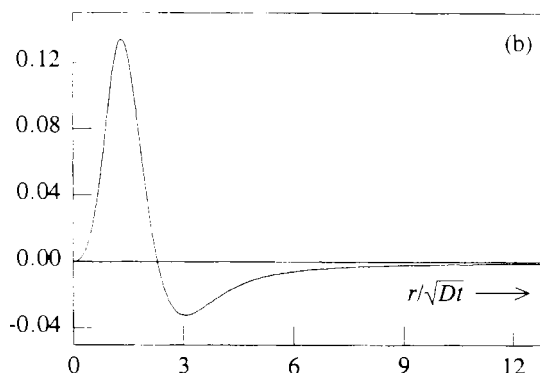

Fig. 5. The product of the normalised currsnt density difference ($i_{cone} - i$ model) plotted versus $r/\sqrt{Dt}$ for semi-apical angles (a) $\theta_0 = 3\pi/4$ and (b) $\theta_0 = \pi/4$. The integration of these functions. see Eq. (47). generated two of the points in Fig 1..

Table 1
Short-time ($r^2 / Dt = 33.6115$) numerical data for a $\theta_0 = 3\pi / 4$ cone and its cylindrical model

$ri_{cone} / FDc^b = 3.73006$ by numerical evaluation of **tq.** (33)
$ri_{model} / FDc^b = 3.72700$ by numerical evaluation of Eq. (46)
Difference 0.00294
First right-hand term in Eq. (51) for $ri_{model} / FDc^b = 3.248345$
Second right-hand term in **Eq.** (51) tor $ri_{model} / FDc^b = 0.500000$
Third right-hand term in Eq. (51) for $ri_{model} / FDc^b = -0.024498$
Fourth right-hand term in **Eq.** (51) tor $ri_{model} / FDc^b = 0.003770$
Sum of first four terms $= 3.727617$

voltammetric behaviour of the cone's model will be to give a current density

$$i_{model} = FDc^b \left[\frac{1}{\sqrt{\pi Dt}} - \frac{\cot \theta_0}{2 r} - \frac{\cot^2 \theta_0}{4 r^2} \sqrt{\frac{Dt}{\pi}} \right.$$
$$\left. - \frac{\cot' \{\theta_0\} Dt}{8 r^3} - \right] \tag{51}$$

It is not obvious that these are the limiting expansions of Eqs. (44) and (45) for large values of $a / \sqrt{Dt}$, but such is indeed the case. Inasmuch as the difference between the currents at an infinite cone and at its infinite cylindrical model are finite and proportional to $\sqrt{t}$, it follows that the currents are identical in the first two terms 0f such an expansion. However, there is strong numerical evidence, that the *third* terms are also identical. Some of this evidence is presented in Tables I and 2. The first thing to notice about these tables is that they show, tor the r^2 / Dt ratios listed. that the sums of the first four terms in Eq. (51) reproduce the exact value of the normalised i_{model} almost perfectly. The second and third important observations are that. in each of the tabulated examples. the magnitude of the normalised difference $i_{cone} - i_{model}$ is decidedly smaller than that of the third term in Eq. (51). and comparable with the magnitude of the fourth term. The strong implication is that the third term in the short-time expansion of i_{cone} is identical to that in i_{model} and that the distinctions between these two expansions lie in their

Table 2
Short-time ($r^2 / Dt = 132.598$) numerical data for a $\theta_0 = \pi / 4$ cone and its cylindrical model

$ri_{cone} / FDc^b = 5.9822$ by numerical evaluation of **tq** (33)
$ri_{model} / FDc^b = 5.9834$ by numerical evaluation of Eq. (46)
Difference -9.0012
First right-hand term in Eq. (51) for $ri_{model} / FDc^b = 6.49670$
Second right-hand term in **Eq.** (51) for $ri_{model} / FDc^b = -0.50000$
Third right-hand term in **Eq.** (51) for $ri_{model} / FDc^b = -0.01225$
Fourth right-hand term in **Eq.** (51) for $ri_{model} / FDc^b = 0.00094$
Sum of first four terms $= 5.98351$

fourth and subsequent terms. Accordingly. we can write the equation for the short-time current density at a cone as

$$i_{cone} = FDc^b \left[\frac{1}{\sqrt{\pi Dt}} - \frac{\cot \theta_0}{3 r} \right.$$
$$\left. - \frac{\cot' \theta_0}{4 r^2} \sqrt{\frac{Dt}{\pi}} + O\left\{ \frac{Dt}{r^3} \right\} \right] \tag{52}$$

9. Computional procedures

The mathematical package MATHEMATICA [43] assisted computation. Values of the Bessel function and its roots. the gamma function. the Kummer function (as its hypergeometric equivalent). the Legendre function and its derivative with respect to argument. and the Neumann function were all evaluated using this assistance. Derivatives of the Legendre function with respect to degree were approximated by $[P_{-\epsilon}\{\mu_0\} - P_{\epsilon}\{\mu_0\}]/2\epsilon$ with $\epsilon = 10^{-3}$. It being carefully ascertained that ϵ values as small as 10^{-7} produced no change in value. The required v_n values were found by MATHEMATICA'S iterative procedure (the secant method). starting with a crude value provided by an approximation formula [44].

Normally only 15 summands were employed in the n-summations, but up to 40 terms were used for performing calculations for 'sharp' cones as the semi-apical angle approached zero or π. The calculation procedure can be considered reliable in the $0.05\pi \le \theta_0 \le 0.90\pi$ range. Convergence was accelerated using the epsilon-algorithm [45] in the version conveniently described (under the name Pade routine') in a mathematical handbook [46].

The inner integration over λ in Eq. (48) was carried out by MATHEMATICA's standard procedure. but this was found to be too slow for the outer integration in Eq. (48) or that in Eq. (49). Consequently. those numerical integrations were usually performed only over the interval $0.01 \le \xi \le 400$. Special care being taken to ensure (with the help of an expanded integration grid) that there were no significant contributions from outside this range. The expanded grid gave better resolution for small ξ values. The integrand was interpolated between calculated values. after which the integration was performed by a standard routine.

10. Summary and discussion

We have studied potential-leap voltammetry at an infinite conical electrode. Our analysis has provided exact information on the concentration and current density responses over the entire time spectrum and at all locations. The general results. embodied in Eqs. (30) and (33), are complicated enough that numerical procedures must be used to investigate their implications. However. we have

also derived transparent expansions. namely those in Eqs. (36) and (52). which describe the current density when the quantity r^2/Dt is either small or large.

Recall that the motivating objective of this research was to identify the magnitude of the $\sqrt{D^3 t}$ term in the short-time current, and observe how this depended on the semi-apical angle θ_0. The arguments leading to Eq. (52) lead us to conclude that the magnitude of the $\sqrt{D^3 t}$ term in the short-time current *density* expression is

$$-\frac{4Fc^{\text{b}}}{r^2}\cot^2\{\theta_0\}\sqrt{\frac{D^3 t}{\pi}} \tag{53}$$

which. when integrated over the entire conical electrode. produces an infinite current. That nonsensical result is not surprising inasmuch as we have seen that there is no meaningful interpretation of 'short-time' at the apex $r = 0$ itself. Moreover, the entire term in Eq. (53) can be interpreted as arising from the curvature of the cone. leaving no contribution whatsoever from the apex!

On reflection, our view is that there is nothing paradoxical in this last result. For the cone. the curvature of the surface is inseparable from the apex: they are both manifestations of the conical geometry. The term in expression (53) may be interpreted as arising either from the presence of the apex. or as a consequence of the curvature. Note that this term is invariably negative (in contrast to the positive contribution revealed in Eq. (1) from the vertex of a hollow cube) and that it acquires large magnitudes when the cone's semi-apical angle is close to the values of 0 and π, signifying spike-shaped cones.

Acknowledgements

References

[1] A.F.S. Afshar. D.R. Gabe and B. Sewell. J. Appl Electrochem.. 21 (1991) 32.

[2] J. Jordan. C.A. Javick and W.E. Ranz. J. Am. Chem. Soc., 80 (1958) 3816.

[3] J. Jordan. C.A. Javick and W.E. Ranz. Anal. Chem.. 27 (1955) 1708.

[4] R.M. Penner. M.J. Heben and N.S. Lewis. Anal. Chem.. 61 (1989) 1630.

[5] A.J. Bard. M.V. Mirkin and C.G. Zoski. Meet. Am. Chem. Soc., August 1993. Vol. 206. Abstr.. p. I21-ANYL.

[6] C.F. Quate. Phys. Today. 39 (1986) 26.

[7] A.J. Bard, F.-R.F. Fan. J. Kwak and O. Lev. Anal. Chcm.. 61 (1989) 132.

[8] K. Aoki and M. Sakai. J. Electroanal. Chem.. 267 (1989) 47.

[9] M.V. Mirkin, F.-R.F. Fan and A.J. Bard. Science. 257 (1992) 364.

[10] P.R. Kennedy. J. Neurosci. Methods. 29 (1989) 181.

[11] P.R. Kennedy. S S Mirra and R.A.E. Bakay. Neurosci. Lett.. 142 (1992) 89.

[12] P.R. Kennedy. R.A.E. Bakay and S.M. Sharpe. Neurosci. Rep.. 3 (1992) 605.

[13] K Aoki. J. Electroanal Chem.. 281 (1990) 29.

[14] J.O. Besenhard. A. Schulte. K. Schur and P.D. Jannakoudakis. in M.1. Montenegro. M.A. Queiros and J.L. Daschhach (Eds.). Microelectrode: Theory and Applications, Kluwer. Dordrecht. Netherland. 1991. p. 189.

[15] T.G. Strein and A.G. Ewing. Anal. Chem.. 64 (1992) 1368.

[16] J.A. Patterson, R. Grief and I. Cornet. Int. J Heat Mass Transfer. 16 (1973) 1017.

[17] R.N. Srnith and R. Grief. Int. J. Heat Mass Transfer. 34 (1975) 1249.

[18] W.-S. Yu. H -T. Lin and T.-Y. Hwang. Int. J. Heat Mass Transfer. 34 (1991) 2197.

[19] 11. Fedchenia. P.-0. Westlund and U. Cegrell. Molec. Sim.. 11 (1993) 373.

[20] V.A. Kozlov Math. USSR Sbornik. 64 (1989) 383

[21] M. Dobrowolski. J.R. Angew Math.. 391 (1993) 185.

[22] M. Bourlard, M Dauge. M.-S. Luhuma and S. Nicaise. SlAM J. Numer. Anal.. 29 (1992) 136.

[23] M.V Borsuk. Math. USSR Shornih. 71 (1993) 185.

[24] K.B. Oldham. J. Electroanal. Chem.. 297 (1991) 317.

[25] J.C. Myland and K.B. Oldham. J. Electroanal. Chem.. 405 (1996) 39.

[26] H.S. Carslaw and J.C. Jaeger. The Conduction of Heat in Solids. Oxford University) Press. Oxford. UK. 2nd edn.. 1959. p. 184.

[27] H.S. Carslaw and J.C. Jaeger. The Conduction of Heat in Solids. Oxford University)Press. Oxford. UK. 2nd edn.. 1959. p. 120.

[28] J Spanier and K.B. Oldham. An Atlas of Functions. Hemisphere, New York/Springer, Berlin, 1987. Eq. .59:3:10.

[29] G.M. Murphy. Ordinary Differential Equations and their Solutions. Van Nostrand, Princeton, NJ. 1960.

[30] J. Spanier and K.B. Oldham. An Atlas of Functions. Hemisphere. New Yorh/Springer, Berlin,1987. Chap. 17.

[31] M. Abramowitz and I.A. Stegun. Handhook of Mathematical Functions. National Bureau of Standards. Washington. DC. 1961. formula 13:I:5.

[32] H.S. Carslaw and J.C. Jaeger. The Conduction of Heat in Solids. Oxford University Press. Oxford. UK. 2nd edn.. 1959. pp. 252-253.

[33] A.V. Sokirko, unpuhlished studies, 1995.

[34] K.B. Oldharn and J.C. Myland. Fundamentals ot Electrochemical Science. Academic Press, San Diego, 1991. p. 234.

[35] K.B. Oldham. unpublished studies. 1996.

[36] H.S. Carslaw and J.C. Jaeger. The Conduction of Hcat in Solids. Oxford Univesity Press. Oxford. UK. 2nd edn., 1959. p. 336.

[37] N.N. Lebedev. J.P. Skalskaya and Ya.S. Ufiyand, Problems of Mathematical Physics, Gos. Isd. TechnikoTeoretichesko) Lit.. Moscow, 1955. p. 175 (in Russian).

[38] H.S. Carslaw and J.C. Jaeger. The Conduction of Hear in Solid\. Oxford University Prcss. Oxford. UK. 2nd edn.. 1959, p 199.

[39] L. Chen. C.L. Colyer. M.G. Kamau, J.C, Myland. K.B. Oldharn and P.G. Symons, Can. J. Chem.. 72 (1994) 836.

[40] J. Spanier and K.B. Oldham. An Atlas of Functions. Hemisphere. Ncw York/Springer, Berlin. 1987. Chap. 51.

[41] J. Spanier and K.B. Oldham. An Atlas of Functions. Hemisphere. New York/Springer, Berlin. 1987. Chap. 52.

[42] J. Spanier and K.B. Oldham. An Atlas of Functions. Hemisphere. New York/Springer. Berlin. 1987. Sect. 52:7.

[43] Wolfram Research Inc., Champaign. IL. 1989.

[44] I.S. Gradshteyn and I.M. Rhyzhik, Tables of Integrals. Series and Products. Academic Press. New York, 1980. formula 8:787.

[45] J Wimp. Sequence Transformations and their Applications. Academic Press. New York. 1981. pp. 138- 146.

[46] J. Spanier and K.B. Oldharn. An Atlas of Functions. Hemisphere. New York/Springer, Berlin. 1987. Sect. 17:13.